

Original Research Article

Elucidation of mechanisms of action of Wei-Sheng-Fang-Yi-Bao-Dan in the treatment of COVID-19 and depression using network pharmacology and molecular docking

Haicheng Han¹, Rui Fang², Dan Wang¹, Yong Yang^{1,3*}, Xiaoqing Fu³, Kangle Rui⁴

¹School of Public Health, Hangzhou Normal University, Hangzhou, ²School of the Integrated Chinese and Western Medicine, Hunan University of Chinese Medicine, Changsha, ³Hangzhou TCM Hospital Affiliated to Zhejiang Chinese Medical University, ⁴Hangzhou Gongshu Hospital of Integrated Traditional and Western Medicine, Hangzhou, China

*For correspondence: **Email:** yyyg1107@sina.com; **Tel:** +86-18958077618

Sent for review: 15 February 2022

Revised accepted: 25 August 2022

Abstract

Purpose: To investigate the mechanisms of action of Wei-Sheng-Fang-Yi-Bao-Dan (WSFYBD) in the treatment of COVID-19 and depression using network pharmacology and molecular docking.

Methods: First, the bioactive components and target genes of WSFYBD were retrieved from TCMSDB database. The relevant gene targets of depression and COVID-19 were obtained from databases. The core WSFYBD genes for treatment were separately obtained by determining gene intersection. Cytoscape 3.8.0 software was used to draw the visual interactive networks. STRING database was employed to construct protein-protein interaction networks, while Gene Ontology (GO), and Kyoto Encyclopedia of Genes and Genomes (KEGG) functional enrichment analyses were used to determine the function and pathway of target genes via a Bioconductor/R. Finally, AutoDockTools software was employed for molecular docking.

Results: A total of 105 potential bio-active components and 35 target genes of WSFYBD for COVID-19 therapy were identified. Also, 1905 GO entries ($p < 0.05$) and 158 related signal pathways ($p < 0.05$) for COVID-19 were obtained. Similarly, 114 potential bio-active components of WSFYBD and 127 potential therapeutic targets of depression were identified. Moreover, 1948 GO entries ($p < 0.05$) and 177 related signal pathways for depression were retrieved ($p < 0.05$). Docking results showed the main bio-active components were closely bound to the core targets.

Conclusion: The mechanisms for treating COVID-19 show that WSFYBD directly acts on SARS-CoV-2 virus to prevent it from entering the host cell, or inhibits virus replication. Secondly, WSFYBD ameliorates depression by acting on key targets that control over-activated cytokines. Therefore, WSFYBD has potentials for the management of COVID-19 and depression.

Keywords: COVID-19, Depression, Wei-Sheng-Fang-Yi-Bao-Dan, Network pharmacology, Molecular docking, Traditional Chinese medicine (TCM)

This is an Open Access article that uses a funding model which does not charge readers or their institutions for access and distributed under the terms of the Creative Commons Attribution License (<http://creativecommons.org/licenses/by/4.0>) and the Budapest Open Access Initiative (<http://www.budapestopenaccessinitiative.org/read>), which permit unrestricted use, distribution, and reproduction in any medium, provided the original work is properly credited.

Tropical Journal of Pharmaceutical Research is indexed by Science Citation Index (SciSearch), Scopus, Web of Science, Chemical Abstracts, Embase, Index Copernicus, EBSCO, African Index Medicus, JournalSeek, Journal Citation Reports/Science Edition, Directory of Open Access Journals (DOAJ), African Journal Online, Bioline International, Open-J-Gate and Pharmacy Abstracts

INTRODUCTION

COVID-19 broke out in Wuhan, China at the end of 2019. Currently, since no effective treatment has been identified, only symptomatic treatment and support therapy are used [1]. Besides, COVID-19 has increased the prevalence of depression. About 20 % asymptomatic or mildly symptomatic carriers of SARS-CoV-2 have depression [2].

For several centuries, Chinese herb-derived medicines have been used for combatting epidemics. When used for treatment of COVID-19, traditional Chinese medicine (TCM) not only increased respiratory function, but also relieves anxiety and depression, thereby enhancing retention of vital functions and quality of life. The TCM formulation, *Wei-Sheng-Fang-Yi-Bao-Dan* (WSFYBD), was first described in the ancient medical text "*Yi-Xue-Zhong-Zhong-Can-Xi-Lu*" written one hundred years ago. It was used to treat cholera and other epidemics, including acute infectious diseases, and it produced significant effectiveness. In addition, as recorded in the book "*Yi-Xue-Zhong-Zhong-Can-Xi-Lu*", WSFYBD is used to treat depression, and has been widely used in clinical practice. COVID-19 is an acute infectious disease that affects multiple organs such as the heart, the digestive tract, and the nervous system. Therefore, WSFYBD is used for treating both COVID-19 and the associated depression. However, the mechanism of action of the drug is unclear.

Network pharmacology is widely used to predict the mechanisms of action of Chinese medicine formulations in line with the "multigene, multitarget and multi-disease" principle [3]. It was used in this research to determine the underlying principle in the use of WSFYBD for the aforesaid treatments. It has been successfully applied to predict the mechanism of TCM used to treat a variety of diseases in recent years.

METHODS

Chemical components and targets of WSFYBD

Using drug-likeness (DL) ≥ 0.18 and oral bioavailability (OB) $\geq 30\%$ as parameters, WSFYBD herbs were searched in the TCMSP database (<https://tcmsp.com/>). The absence of an active component in a herb was further confirmed through relevant literature. Then, the matching targets of the active compounds were identified, and annotation of target genes was done in UniProt archives (<https://www.uniprot.org/>), with "Homo sapiens" as species.

Target genes of COVID-19 and depression

The illness-associated archives (i.e. OMIM, GeneCards and PharmGKB) were used to identify target genes of COVID-19, with "COVID-19" as the keyword. Similarly, disease-related genes of depression were obtained, with "depression" as the keyword.

Generation of regulative and protein-protein association (PPA) webworks

The matching of targets of elucidated active ingredients with those of COVID-19 was done with R language. Then, genes at the intersections were identified, and putative quarries of WSFYBD in COVID-19 treatment were obtained. Similarly, the potential targets of WSFYBD in depression treatment were obtained. These potential targets and the relationship amongst disease, targets, and bio-active components were inputted into Cytoscape 3.8.0 for visual analysis. The above potential targets, the relationship between disease, targets and bioactive components were inputted into the software, and the regulatory network diagram of "drugs-active components-disease targets" was generated. Adjustments were made on grid hue and configuration on the basis of nodal attributes.

The potential therapeutic targets were loaded into the STRING (<https://string-db.org/>) web platform, with the study species as "Homo sapiens." The top-most score on dependability (≥ 0.4) was chosen, individual targets were concealed, mesh work of PPA was plotted, and the resultant TSV folder was inputted into Cytoscape 3.8.0. Then, CytoNCA plug-in was used for topological analysis. The key gene meshwork was produced on the basis of standard parameters such as betweenness, proximity, intensity, and eigenvector.

Similarly, a meshwork diagram of "drugs-active components-disease targets", the core gene network of WSFYBD in treatment of depression was obtained with the topmost highest reliability score (≥ 0.9) out of a full-scale score.

Analysis of GO and KEGG route enhancement

The GO function and KEGG pathway enrichment analyses were used to separately analyse the potential targets for the treatment of COVID-19 and depression via the Bioconductor package and R parlance. Relevant tables of GO and KEGG route enhancement analyses were derived based on the related scripts of the R parlance. The highest ten indexes of biochemical

process, cell composition and molecular activity were chosen for imaging for analyzing Gene Ontology [4].

Molecular docking

The core genes or key proteins served as receptors in molecular docking, while their related bio-active components in the regulatory networks acted as ligands. AutoDock vina software was used for molecular docking. Then, the docking models with the lowest binding energy (expressed in kcal/mol) were selected and visualized [4].

Ethical approval and consent to participate

The Declaration of Helsinki and national and international guidelines for human research were followed in this study [5]. The study was approved by the Ethics Committee of Hangzhou Gongshu Hospital of Integrated Traditional and Western Medicine (approval no. 202201002).

RESULTS

Major components of WSFYBD and treatment targets

A total of 124 major active components were identified in WSFYBD, including 92 components from Licorice, 8 components from Asari Radix Et Rhizoma, 22 components from *A. dahurica* (Fisch.) Benth, and 3 components from *Borneolum syntheticum*. Both Asari Radix Et Rhizoma and licorice contained kaempferol. Following a search on the TCMSP database, no active component was found in Cinnabar and Bohebing.

Bohebing, also called menthol, had an OB value of 43.31 % and a DL value of only 0.03, based on TCMSP database. The probability of a compound being a drug is designated as DL, while menthol has been widely used in medicine and food industry. Moreover, the DL properties of a compound can be determined via the Lipinski's Rule of Five, and the structure of Bohebing conformed to the Lipinski's Rule of Five, indicating that it is an active component [5]. Therefore, 125 bioactive components of WSFYBD (Table 1), and 158 target genes were obtained via UniProt gene annotation.

A total of 809 COVID-19 disease targets were obtained, as shown in Figure 1 A. A total of 35 cross-genes were obtained by matching the targets of WSFYBD with COVID-19-related targets (Figure 1 B). Similarly, 8180 depression

disease targets (Figure 1 C) and 127 cross-genes (Figure 1 D) were obtained.

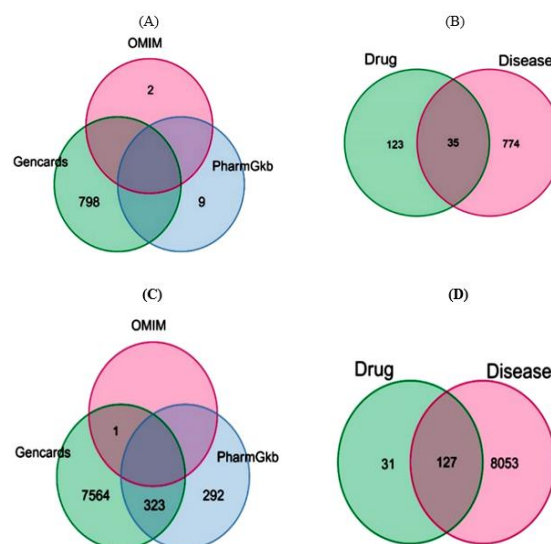


Figure 1: Venn diagrams (VDM) of (A): COVID-19 targets, (B): WSFYBD and COVID-19 targets, (C): Depression target, (D): WSFYBD and depression targets

Regulatory and PPA grid

The obtained regulatory network diagram of COVID-19 and depression are shown in Figure 2 and Figure 3, respectively. The COVID-19 regulatory network had 105 active components, 35 potential therapeutic targets, and 567 edges. Based on degree value, licochalcone A (degree = 15), kaempferol (degree = 15), naringenin (degree = 12), formononetin (degree = 10), and isorhamnetin (degree = 10) were the top 5 active components.

The potential therapeutic genes for COVID-19 obtained were loaded into STRING web platform. A PPI meshwork diagram was obtained (35 nodes and 291 connections; Figure 4 A). For each factor, a median level was then calculated. A total of 13 targets were obtained (Figure 4 B), indicating that they are the core genes involved in COVID-19 treatment with WSFYBD. The meshwork representation of depression control had 114 active components, 127 putative sites, and 1193 edges. Based on the degree values, kaempferol (degree = 46), 7-methoxym-2-methyl isoflavone (degree = 29), beta-sitosterol (degree = 27), naringenin (degree = 26), and licochalcone a (degree = 25) were the top 5 active components.

Similarly, the PPI network diagram related to depression was obtained, with 102 nodes and 305 connections (Figure 4 C). The 7 nodes were

Table 1: Active chemical components of WSFYBD

Herb	Bio-active compound
Licorice	Inermine, Liquiritigenin, Betulinic acid, Calycosin, Kumatakenin, Naringenin, Formononetin, 3-Epi-Beta-Sitosterol, Euchrenone, 7-Methoxy-2-methyl isoflavone, Isorhamnetin, Glycyrol, Kaempferol, Medicarpin, Shinflavanone, Lupiwighteone, Glyasperin C, Isotrifoliol, Glyasperin B, Glyasperin F, Kanzonol B, Semilicoisoflavone B, (2S)-6-(2,4-Dihydroxyphenyl)-2-(2-hydroxypropan-2-yl)-4-methoxy-2,3-dihydrofuro (3,2-g) chromen-7-one, Kanzonols W, Phaseolinisoflavan, Glepidotin B, Glepidotin A, Glypallichalcone, Kanzonol U, Licochalcone B, Licochalcone G, Licoarylcoumarin, Licoricone, Licorice glycoside E, Gancaonin B, Gancaonin A, Gancaonin L, Gancaonin M, 6-Prenylluteolin, Glycyrin, Licocoumarone, Licoisoflavone B, Licoisoflavone, Shinpterocarpin, Licoisoflavanone, 5-Prenylbutein, Licopyranocoumarin, Liquiritin, 3,22-Dihydroxy-11-oxo-delta (12)-oleanene-27-alpha-methoxycarbonyl-29-oic acid, Glabrone, Glabranin, Glabridin, Glabrene, Glyzaglabrin, Hedysarimcoumestan B, 1,3-Dihydroxy-8,9-dimethoxy-(1) benzofuro (3,2-c) chromen-6-one, (-)-Medicocarpin, Glycyroside, Eurycarpin A, Sigmoidin-B, (2R)-7-hydroxy-2-(4-hydroxyphenyl) chroman-4-one, Isobavachin, Quercetin der, Isolicoflavonol, 1-Methoxyphaseollidin, HMO, Isoglycyrol, 3'-Hydroxy-4'-O-Methylglabridin, 3'-Methoxyglabridin, Licochalcone a, 4'-Methoxyglabridin, Kanzonol F, Icos-5-enoic acid, Inflacoumarin A, 7,2',4'-trihydroxy-5-methoxy-3-arylcoumarin, 6-prenylated eriodictyol, Vestitol, 8-prenylated eriodictyol, Gadelaidic acid, 7-Acetoxy-2-ethylisoflavone, Xambioona, Licoagrocarpin, Gancaonin H, Licoagrisoflavone, Odoratin, Glyasperins M, 18 α -hydroxyglycyrrhetic acid, Glycyrrhiza flavonol A, Phaseol, Gancaonin G, Dehydroglyasperins C, Quercetin
<i>Asari radix</i> Et Rhizoma	4,9-Dimethoxy-1-vinyl-beta-carboline, Sesamin, Cryptopin, Caribine, (1R,3R)-3-((E)-3-Methoxy-2-methyl-3-oxo-1-propenyl)-2,2-dimethylcyclopropanecarboxylic acid (S)-3-(2-butenyl)-2-methyl-4-oxo-2-cyclopenten-1-yl, 3-O-methylviolanone, ZINC05223929, Kaempferol
<i>A. dahurica</i> (Fisch.) Benth. Et Hook 1	Ammidin, Alloisoimperatorin, Mandenol, Isoimperatorin, Neobyakangelico I, Byakangelicol, Cnidilin, Pabulenol, Ethyl oleate (NF), CLR, 4-((2S)-2,3-dihydroxy-3-methylbutoxy) furo (3,2-g) chromen-7-one, Stigmasterol, Beta-sitosterol, Senbyakangelicol, Propyleneglycol monoleate, Phellopterin, ZINC03860434, Supraene, Prangenidin, 2-Linoleoylglycerol, Methyl icoso-11,14-dienoate, Prangenin, Asiatic acid, Bronyl acetate, Dipterocarpol, Menthol
<i>Borneolum Syntheticum</i>	
Bohebing	

obtained after two rounds of screening (Figure 4 D).

GO function and KEGG pathway enrichment analyses

A GO function analysis was performed on the 35 target genes shared between the active components of WSFYBD and COVID-19, resulting in 1905 GO entries ($p < 0.05$). Figure 5 A, depicts ten principal indices chosen for imaging. The KEGG pathway enrichment analysis identified 158 related signal routes associated with COVID-19 treatment with WSFYBD. Thirty key parameters were subjected to visual assessment (Figure 5 B).

Similarly, GO function analysis was performed on 127 gene targets shared between active components of WSFYBD and depression ($p < 0.05$). A total of 1948 GO entries were obtained

(Figure 5 C). Then, 177 associated signal routes linked with WSFYBD in the treatment of depression were obtained via KEGG pathway enrichment analysis, and thirty key routes were subjected to visual assessment (Figure 5 D).

Molecular docking

Angiotensin-converting enzyme 2 (ACE2; PDB ID: 1R42) and 3-chymotrypsin-like cysteine protease (3CL pro; PDB ID: 6LU7) were used as the targets for docking with the active components of WSFYBD [6].

The active components of the prescription with degree values greater than the median value were selected for docking, based on the regulatory network diagram (Figure 2 and Figure 3).

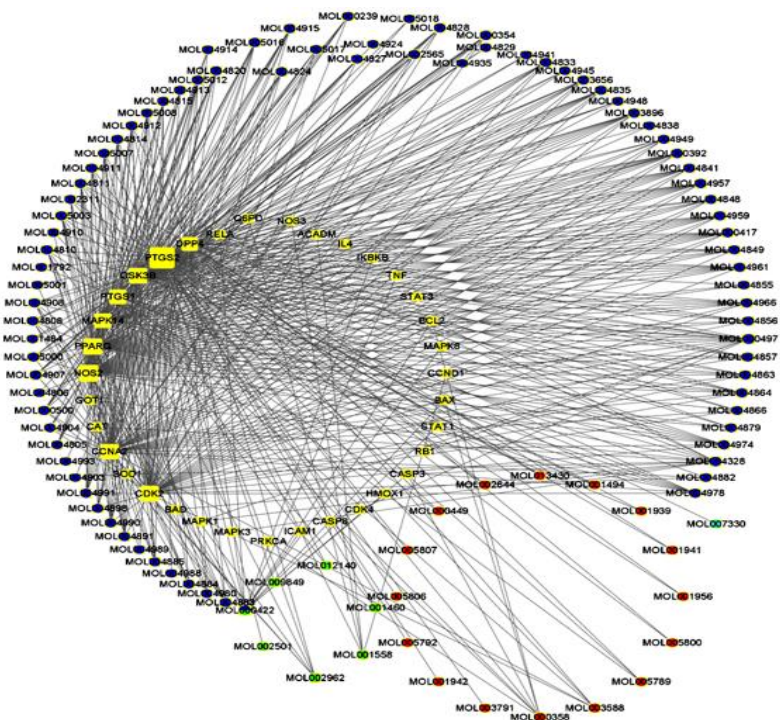


Figure 2: The "drug-bioactive component-disease target" network for COVID-19. The dark blue, red, light green and light blue circles represent licorice, *A. dahurica* (Fisch.) Benth. Et Hook, *Asari radix* Et Rhizoma, and Bohebing, respectively

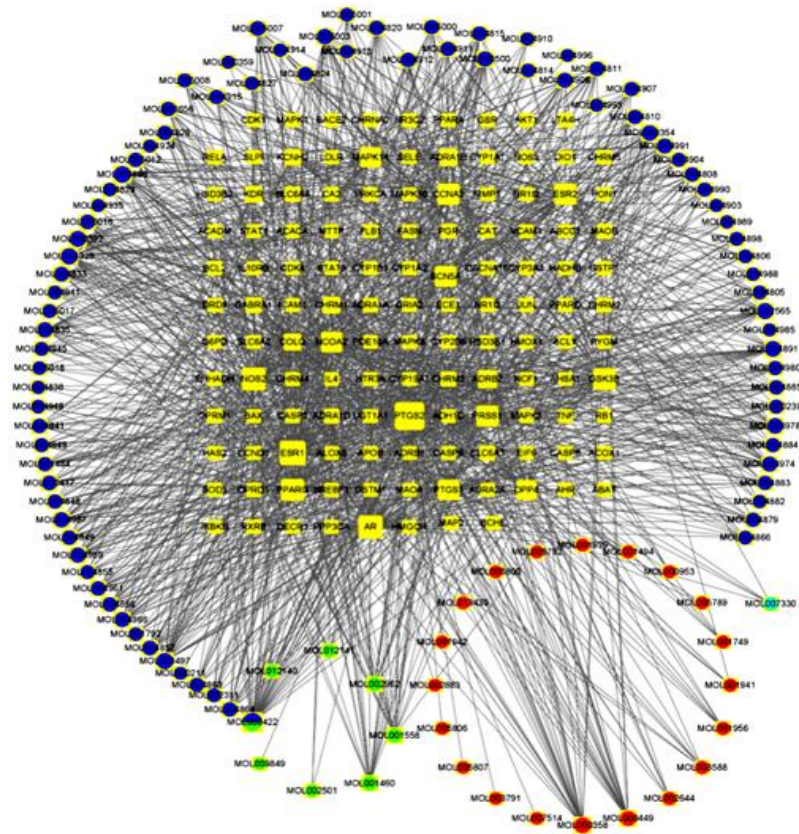


Figure 3: The "drug-bioactive components-disease target" network for depression. The dark blue, red, light green and light blue circles indicate licorice, *A. dahurica* d (Fisch.) Benth. Et Hook, *Asari radix* Et Rhizoma, and Bohebing, respectively.

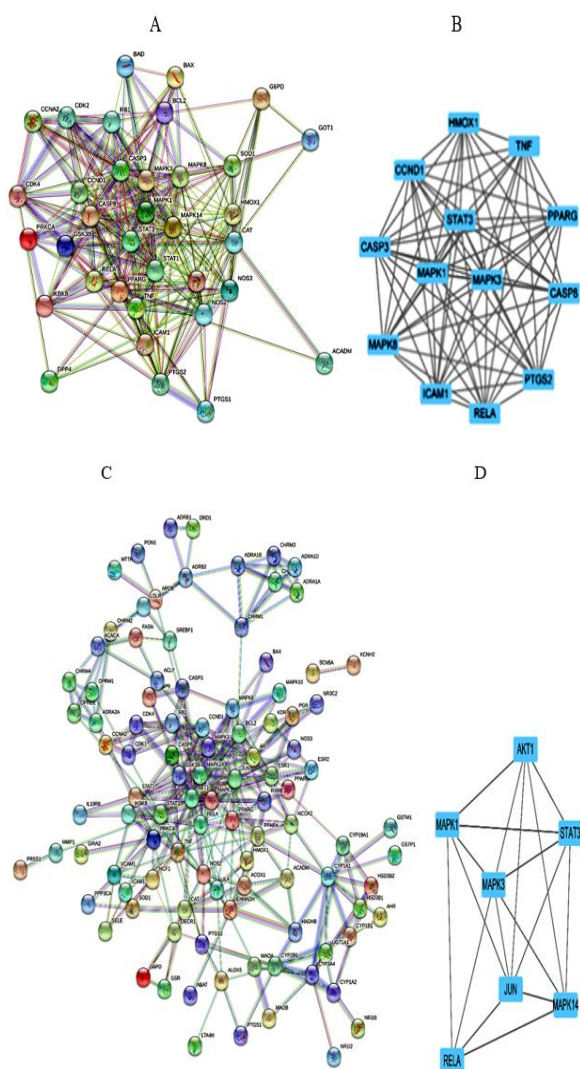


Figure 4: (A) PPI network for COVID-19, (B) Core genes of COVID-19, (C) PPI meshwork for depression, (D) Major genes of depression

Lopinavir, Remdesivir, Ritonavir, Arbidol, Favipiravir, Chloroquine, and hydroxychloroquine were used as references, based on literature. The results are shown in Table 2 and Table 3. The smaller the value, the deeper the green, and the larger the value, the deeper the red. All the energy levels of the molecular docking results were less than -5 kcal/mol, indicating that the active components have research value and may be the key components involved in the treatment of COVID-19 [7]. The docking scores of licoisoflavone, shinpterocarpin, and glyasperin F were less than those of the recommended standard drugs such as remdesivir and ritonavir. This indicates that they have stronger binding power than the recommended drugs, and that they may be useful in further research. The molecular docking diagrams are shown in Figure 6 and Figure 7.

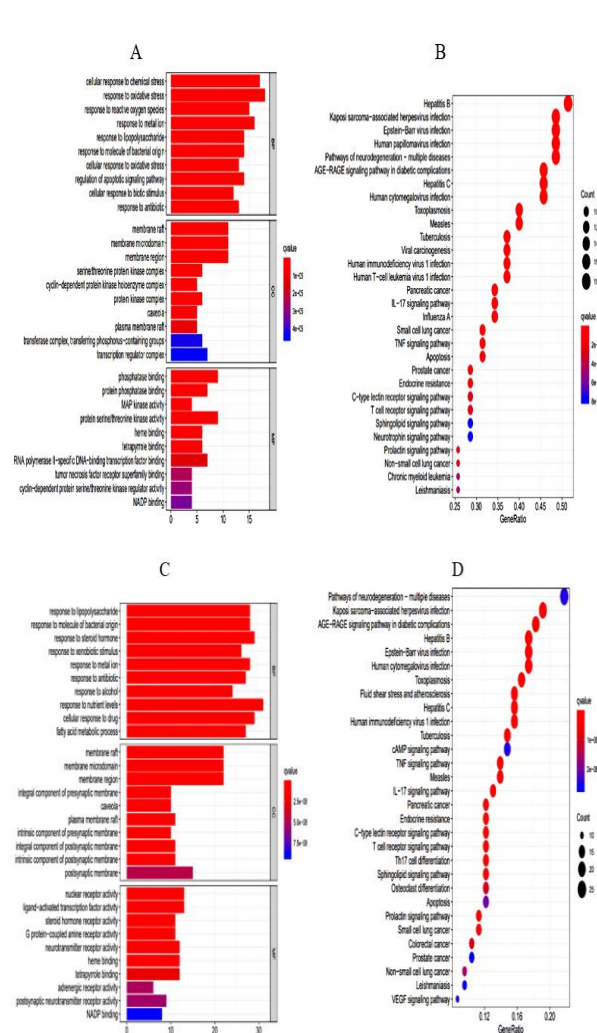


Figure 5: (A) GO function analysis for COVID-19, (B) KEGG pathway analysis for COVID-19, (C) GO function analysis of depression, (D) KEGG pathway analysis for depression

However, it is difficult to determine which protein is key in the pathogenesis of depression. Therefore, the 7 core proteins and genes in Figure 4 D were used as docking targets during molecular docking. For small-molecule ligands, all the active components connected to the 7 core genes were docked with the core proteins, based on the regulatory network diagram in Figure 2 and Figure 3.

All the docking scores were less than -5 kcal/mol, and the docking score of each of the components kanzonols W, shinpterocarpin, glabrene, glabridin, and MAPK14 was less than -10 kcal/mol (Table 3). Overall, these results show that WSFYBD acts on related genes via the above-mentioned active components in the treatment of depression.

Table 2: Molecular docking results of COVID-19

Component	Docking score (kcal/mol)	
	ACE2	3CLPro
Licochalcone A	-8	-6.4
Kaempferol	-7.6	-6.9
Naringenin	-7.6	-6.8
Formononetin	-7.5	-7.2
Isorhamnetin	-7.6	-6.6
Odoratin	-7.6	-6.8
Vestitol	-7.3	-6
HMO	-7.7	-6.5
Glabrone	-8.1	-7.2
Glyzaglabrin	-7.8	-7.2
Glepidotin A	-8.3	-6.7
Calycosin	-7.4	-6.6
7-Methoxy-2-methyl isoflavone	-7.3	-6.6
Licoagroisoflavone	-8.1	-7.2
Licoagrocarpin	-8.4	-7.6
7-Acetoxy-2-methylisoflavone	-7.5	-6.5
7,2',4'-trihydroxy-5-methoxy-3-arylcoumarin	-7.8	-6.9
4'-Methoxyglabridin	-8.2	-6.7
3'-Methoxyglabridin	-8.1	-7.0
3'-Hydroxy-4'-O-Methylglabridin	-8	-7.1
Quercetin der	-7.5	-6.7
1-Methoxyphaseollidin	-7.7	-6.6
Eurycarpin A	-8.2	-6.9
Shinpterocarpin	-9.2	-7.5
Gancaonin M	-8.4	-7.9
Licochalcone B	-7.3	-7.0
Glypallichalcone	-7.2	-6.2
(2S)-6-(2,4-dihydroxyphenyl)-2-(2-hydroxypropan-2-yl)-4-methoxy-2,3-dihydrofuro[3,2-g]chromen-7-one	-8.2	-7.1
kanzonols W	-8.5	-7.8
Kanzonol B	-8.3	-7.1
Glyasperin C	-8	-7.2
Glyasperin F	-8.7	-7.4
Lupiwighteone	-8.4	-7.8
Glyasperins M	-8.3	-7.5
Gancaonin G	-7.6	-6.7
Glabrene	-8.5	-7.3
Glabridin	-8	-7.1
Licoisoflavanone	-8.5	-7.2
Licoisoflavone	-9.3	-7.3
Gancaonin L	-8.2	-7.9
Licoarylcoumarin	-7.9	-6.8
Licochalcone G	-7.9	-6.3
Phaseolinisoflavan	-8	-7.4
Glyasperin B	-8.1	-7.1
Beta-sitosterol	-7.6	-6.9
Lopinavir	-8.1	-7.4
Remdesivir	-8.4	-6.8
Ritonavir	-8.4	-7.0
Arbidol	-6.9	-5.7
Favipiravir	-5.6	-5.8
Chloroquine	-6.3	-5.4
Hydroxychloroquine	-6.7	-5.4

Table 3: Molecular docking results of depression

Gene/ Protein	Components	Docking score (kcal/mol)
STAT3	Licochalcone A	-6.5
MAPK3	Naringenin	-9.3
MAPK14	Glycyrol	-8.9
MAPK14	Isorhamnetin	-8.8
MAPK14	Lupiwighteone	-9.1
MAPK14	7-Methoxy-2-methyl isoflavone	-9.1
MAPK14	Formononetin	-8.9
MAPK14	Calycosin	-9.5
MAPK14	Shinflanvanone	-9.8
MAPK14	Glyasperin F	-9.3
MAPK14	Glyasperin C	-8.4
MAPK14	Isotrifoliol	-8.7
MAPK14	Kanzonol B	-9.3
MAPK14	Kanzonols W	-10.8
MAPK14	(2S)-6-(2,4-dihydroxyphenyl)-2-(2-hydroxypropan-2-yl)-4-methoxy-2,3-dihydrofuro[3,2-g]chromen-7-one	-9.6
MAPK14	Glepidotin A	-9.4
MAPK14	Phaseolinisoflavan	-9.5
MAPK14	Glypallichalcone	-8.2
MAPK14	Licochalcone B	-8.6
MAPK14	Licochalcone G	-8.6
MAPK14	Licoarylcoumarin	-9.5
MAPK14	Gancaonin L	-8.9
MAPK14	Gancaonin M	-9
MAPK14	Licoisoflavone	-8.9
MAPK14	Shinpterocarpin	-10.4
MAPK14	5-Prenylbutein	-9
MAPK14	Glyzaglabrin	-9.6
MAPK14	Glabridin	-10.2
MAPK14	Glabrene	-10.3
MAPK14	Glabrone	-9.6
MAPK14	Hedysarimcoumestan B	-8.8
MAPK14	1,3-Dihydroxy-8,9-dimethoxy-[1]benzofuro[3,2-c]chromen-6-one	-8.3
MAPK14	Eurycarpin A	-8.4
MAPK14	HMO	-9
MAPK14	1-Methoxyphaseollidin	-8.7
MAPK14	Quercetin der	-8.7
MAPK14	3'-Hydroxy-4'-O-Methylglabridin	-10
MAPK14	Licochalcone A	-8.4
MAPK14	3'-Methoxyglabridin	-8.6
MAPK14	4'-Methoxyglabridin	-9.6
MAPK14	ZINC105741014	-9.1
MAPK14	7-Acetoxy-2-methylisoflavone	-9.1
MAPK14	Vestitol	-8.3
MAPK14	Gancaonin G	-9.2
MAPK14	Licoagrocarpin	-8.6
MAPK14	Licoagroisoflavone	-9.4
MAPK14	Odoratin	-9.2
MAPK14	Phaseol	-9.4
AKT1	Kaempferol	-7.6
AKT1	Naringenin	-8.0
JUN	Beta-Sitosterol	-7.2
JUN	Formononetin	-8.0
JUN	Kaempferol	-9.2
RELA	Kaempferol	-7.1
RELA	Naringenin	-7.2
RELA	Licochalcone a	-7.4
RELA	Isorhamnetin	-7.1
MAPK1	Naringenin	-7.4
MAPK1	Licochalcone A	-7.5

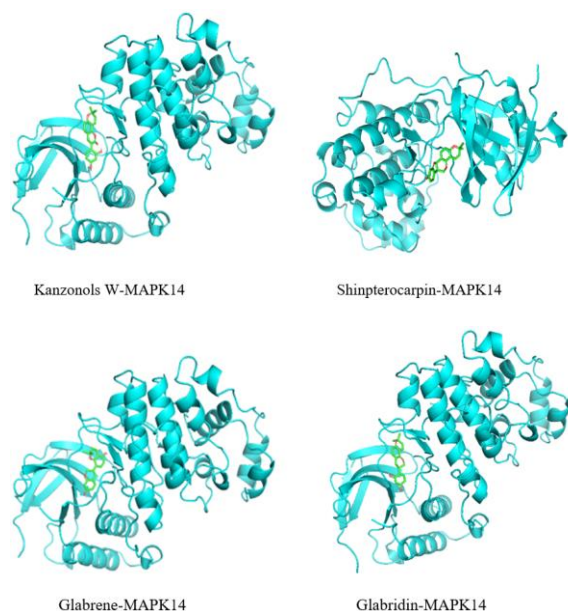


Figure 7: Molecular docking for depression

DISCUSSION

The prescriptions of TCM are usually based on the principle of "Jun-Chen-Zuo-Shi" ("Monarch-Minister-Assistant-Courier") [8]. Based on the book "Yi-Xue-Zhong-Zhong-Can-Xi-Lv", the components of WSFYBD were licorice (300 g), *Asari radix* Et Rhizoma (45 g), *A. dahurica* (Fisch.) Benth. Et Hook (30 g), Bohebing (12 g), *Borneolum syntheticum* (6 g) and Cinnabar (90 g). Licorice is regarded as the 'Monarch' herb based on the order and dose. According to traditional Chinese medicine theory, licorice reinforces *qi*, clears heat, has detoxification effects, expels phlegm, stops cough and alleviates pain. Pharmacological studies have also found that licorice exerts anti-microbial, antiviral, anti-tumor, immune-regulatory and anti-depressant effects [9]. *Asari radix* Et Rhizoma, and *A. Dahurica D* (Fisch.) Benth. Et Hook are minister herbs that help the monarch herb treat the main symptoms. Bohebing and *Borneolum syntheticum*, together with Cinnabar, are assistant herbs and courier herbs which enhance the therapeutic effects of other herbs, enabling them to reach the disease location. Recent studies have also shown that *Borneolum syntheticum* enhanced the capacity of other drugs to penetrate the blood-brain barrier, consistent with the role of courier herb in TCM [10]. Moreover, the proportion of potential active components reflect the principle of "Jun-Chen-Zuo-Shi" based on the preliminary screening of OB and DL, and the regulatory network diagrams. For instance, the results from preliminary screening showed that the proportions of active components in Monarch,

Minister, and Assistant-cum-Courier herbs were 73.60 % (92/125), 24 % (30/125), and 3.20 % (4/125), respectively. These results indicate that in WSFYBD, licorice plays a major and critical therapeutic role by fully exerting its antiviral, antidepressant and immunomodulatory effects.

In previous studies, active components of high-degree values based on regulatory network diagrams were also related to anti-infection and anti-depression. Licochalcone A exerts anti-inflammatory and anti-oxidant effects, inhibits inflammatory response in macrophages, and reduces the secretion of inflammatory cytokines [11]. Kaempferol has a broad-spectrum anti-inflammatory effect, and it alleviates inflammation by regulating various signalling pathways. Animal experiments have shown that Naringin relieves symptoms of depression by modulating oxido-inflammatory insults and NF- κ B/BDNF expressions [12]. Studies have also shown that beta-sitosterol mitigates depression.

There are two possible therapeutic mechanisms involved in the therapeutic effects of WSFYBD on COVID-19: direct action on the SARS-CoV-2 virus, and immune-regulation and anti-inflammation. This study has shown that many active components of WSFYBD produced good docking results with ACE2 or 3CL pro, indicating good interactions. For instance, the docking scores of licoisoflavone, shinpterocarpinols, and glyaspering F were better than those of recommended standard drugs. Therefore, these active components can directly inhibit SARS-CoV-2 replication by controlling ACE2 and 3CL pro.

When SARS-CoV-2 binds to alveolar epithelial cells, it activates both innate and adaptive immunity, releasing a large number of cytokines. However, excessive cytokines trigger a "cytokine storm", and several secondary secretions block the airway, leading to edema, hypoxia, and targeted organ damage which can lead to progression of COVID-19 and even death [13].

The core genes obtained from PPI included *pparg*, *icam1*, *tnf*, *ccnd1*, *hmx1*, *ptgs2*, *mapk8*, *casp8*, *rela*, *casp3*, *mapk3*, *stat3* and *mapk1*. Animal experiments have shown that *pparg* gene regulates lung inflammation, disease development during respiratory viral infection, and restoration of tissue homeostasis after infection [14]. The *icam1* gene regulates inflammation, while *tnf* gene is a key mediator and regulator of the mammalian immune response. The *ccnd1* gene regulates cell proliferation. High-throughput screening experiments have shown that the reading frame

3a (ORF3a) protein of SARS-CoV-2 virus binds to human HMOX1 protein. Some potential therapeutic drugs exert anti-viral efficacy and control 'cytokine storms' by adjusting this combination [15]. The *ptgs2* gene also regulates acute inflammation. The genes *mapk1*, *mapk3*, and *mapk8* regulate the production of inflammatory mediators and control tissue homeostasis, while *casp3* and *casp8* genes prevent the production of "cytokine storm" during viral infection by regulating cytokine release [16]. The *rela* gene plays a key role in the activation and maintenance of regulatory T Cell during infections, while *stat3* gene induces pro-inflammatory or anti-inflammatory responses during inflammatory immune response. Therefore, most of the core genes obtained are related to anti-inflammatory and immune regulation. The KEGG enrichment analysis showed that most of the signal pathways were related to infection and immunity, similar to the mechanism of most Chinese herbal compounds used for COVID-19 treatment.

Many studies have shown that changes in the internal environment of the peripheral immune system and excessive activation of pro-inflammatory cytokines are the major causes of mood disorders such as depression and anxiety. Infections cause continuous activation of the peripheral immune system, and the excessively activated cytokines promote the development of depressive symptoms. Therefore, control of over-activated cytokines through immune regulation could ameliorate depression symptoms associated with inflammation-related diseases [17].

With respect to the core genes of depression in this study, genetic polymorphism involving *akt* and *akt1* is associated with susceptibility to psychiatric disorders such as depression and anxiety. The genes *stat3*, *mapk3*, *mapk14*, *rela*, *jun* and *mapk1* are related to inflammation and immunity. Most of the signal pathways are also related to immunity, infection, and nervous system, based on KEGG enrichment analysis. The MAPK signal pathway regulates the persistence of immune response in activated T cells and CD95-mediated apoptosis in inflammatory responses [18]. The docking scores were all less than -5 kcal/mol. In particular, the scores for kanzonolsk W, Shinpterocarpin, glabrene, glabriding, and MAPK14 were all less than -10 kcal/mol, indicating that these active components have a very strong binding potential to the core proteins. Therefore, these potential active components may also act on the above-mentioned core genes to inhibit the release of proinflammatory cytokines and control over-

activated cytokines, thereby alleviating depressive symptoms.

CONCLUSION

This study has shown that WSFYBD alleviates depression by acting on key targets, thereby inhibiting the release of proinflammatory cytokines and controlling over-activated cytokines. There are two mechanisms involved in the use of WSFYBD for treating COVID-19: the potential active components directly act on the SARS-CoV-2 virus and prevent the virus from entering the host cell, or inhibit viral replication. Secondly, it regulates immunity, controls over-activation of cytokines and decreases cytokine storms. In addition, WSFYBD produces multi-component, multitarget, and multi-pathway interactive effects. It consists of relatively few herbs and it has a wide therapeutic range, thereby justifying its current use in clinical practice in China.

DECLARATIONS

Acknowledgements

None provided.

Funding

This study was supported by Science and Technology Development Program of Hangzhou (no. 20180417A03), and Traditional Chinese Medicine Science and Technology Plan of Zhejiang Province (no. 2020ZB202) in China.

Availability of data and materials

The datasets used and/or analyzed during the current study are available from the corresponding author on reasonable request.

Conflict of interest

No conflict of interest is associated with this work.

Contribution of authors

We declare that this work was done by the authors named in this article, and all liabilities pertaining to claims relating to the content of this article will be borne by the authors. Haicheng Han and Rui Fang conceived and designed the study, and drafted the manuscript. Haicheng Han, Rui Fang, Dan Wang, Yong Yang, Xiaoqing Fu collected, analysed and interpreted the data. Rui Fang, Dan Wang and Kangle Rui revised the

manuscript for important intellectual content. All authors read and approved the final manuscript.

Open Access

This is an Open Access article that uses a funding model which does not charge readers or their institutions for access and distributed under the terms of the Creative Commons Attribution License (<http://creativecommons.org/licenses/by/4.0>) and the Budapest Open Access Initiative (<http://www.budapestopenaccessinitiative.org/read>), which permit unrestricted use, distribution, and reproduction in any medium, provided the original work is properly credited.

REFERENCES

1. Wang R, Luo X, Liu F, Luo S. Confronting the threat of SARS-CoV-2: Realities, challenges and therapeutic strategies (Review). *Exp Ther Med* 2021; 21: 155-171.
2. Jeong SJ, Chung WS, Sohn Y, Hyun JH, Baek YJ, Cho Y, Kim JH, Ahn JY, Choi JY, Yeom JS. Clinical characteristics and online mental health care of asymptomatic or mildly symptomatic patients with coronavirus disease 2019. *PLoS One* 2020; 15: e0242130.
3. Zhang L, Lu S, Hu Z, Liao M, Li C, Kong S. Prediction of the anti-inflammatory effects of bioactive components of a Hippocampus species-based TCM formulation on chronic kidney disease using network pharmacology. *Trop J Pharm Res* 2021; 20(11): 2355-2362.
4. Feng C, Zhao M, Jiang L, Hu Z, Fan X. Mechanism of modified danggui sini decoction for knee osteoarthritis based on network pharmacology and molecular docking. *Evid Based Complement Alternat Med* 2021; 2: 6680637.
5. Dong J, Wang NN, Yao ZJ, Zhang L, Cheng Y, Ouyang D, Lu AP, Cao DS. ADMETlab: A platform for systematic ADMET evaluation based on a comprehensively collected ADMET database. *J Cheminform* 2018; 10: 29-39.
6. Wrapp D, Wang N, Corbett KS, Goldsmith JA, Hsieh CL, Abiona O, Graham BS, McLellan JS. Cryo-EM structure of the 2019-nCoV spike in the prefusion conformation. *Sci* 2020; 367: 1260-1263.
7. Castro-Alvarez A, Costa AM, Vilarrasa J. The performance of several docking programs at reproducing protein-macrolide-like crystal structures. *Molecules* 2017; 22: 136-149.
8. Ji S, He DD, Su ZY, Du Y, Wang YJ, Gao SK, Guo MZ, Tang DQ. P450 enzymes-based metabolic interactions between monarch drugs and the other constituent herbs: A strategy to explore compatibility mechanism of Sangju-Yin. *Phytomed* 2019; 58: 152866.
9. Jiang M, Zhao S, Yang S, Lin X, He X, Wei X, Song Q, Li R, Fu C, Zhang J, et al. An "essential herbal medicine"-licorice: A review of phytochemicals and its effects in combination preparations. *J Ethnopharmacol* 2020; 249: 112439.
10. Hou T, Li X, Peng C. Borneol enhances the antidepressant effects of asiaticoside by promoting its distribution into the brain. *Neurosci Lett* 2017; 646: 56-61.
11. Furusawa J, Funakoshi-Tago M, Mashino T, Tago K, Inoue H, Sonoda Y, Kasahara T. Glycyrrhiza inflata-derived chalcones, Licochalcone A, Licochalcone B and Licochalcone D, inhibit phosphorylation of NF-kappaB p65 in LPS signaling pathway. *Int Immunopharmacol* 2009; 9: 499-507.
12. Olugbemide AS, Ben-Azu B, Bakre AG, Ajayi AM, Femi-Akinlosotu O, Umukoro S. Naringenin improves depressive- and anxiety-like behaviors in mice exposed to repeated hypoxic stress through modulation of oxidoinflammatory mediators and NF-kB/BDNF expressions. *Brain Res Bull* 2021; 169: 214-227.
13. Xu Z, Shi L, Wang Y, Zhang J, Huang L, Zhang C, Liu S, Zhao P, Liu H, Zhu L, et al. Pathological findings of COVID-19 associated with acute respiratory distress syndrome. *Lancet Respir Med* 2020; 8: 420-422.
14. Huang S, Zhu B, Cheon IS, Goplen NP, Jiang L, Zhang R, Peebles RS, Mack M, Kaplan MH, Limper AH, et al. PPAR-γ in macrophages limits pulmonary inflammation and promotes host recovery following respiratory viral infection. *J Virol* 2019; 93: e00030-00019.
15. Batra N, De Souza C, Batra J, Raetz AG, Yu AM. The HMOX1 Pathway as a promising target for the treatment and prevention of SARS-CoV-2 of 2019 (COVID-19). *Int J Mol Sci* 2020; 21: 1-16.
16. Ning X, Wang Y, Jing M, Sha M, Lv M, Gao P, Zhang R, Huang X, Feng JM, Jiang Z. Apoptotic caspases suppress type I interferon production via the cleavage of cGAS, MAVS, and IRF3. *Mol Cell* 2019; 74: 19-31.
17. Ménard C, Hodes GE, Russo SJ. Pathogenesis of depression: Insights from human and rodent studies. *Neurosci* 2016; 321: 138-162.
18. Holmström TH, Schmitz I, Söderström TS, Poukkula M, Johnson VL, Chow SC, Krammer PH, Eriksson JE. MAPK/ERK signaling in activated T cells inhibits CD95/Fas-mediated apoptosis downstream of DISC assembly. *Embo J* 2000; 19: 5418-5428.